Computer and Information Science; Vol. 17, No. 2; 2024
ISSN 1913-8989 E-ISSN 1913-8997
Published by Canadian Center of Science and Education

Study of the Simulation and Application of the PEEC Method for Modeling the Prediction of Emissions Radiated by the Onboard Electronic Wiring System

Anthony Bassesuka Sandoka Nzao[1]

[1] ISTA Kinshasa, Electrical Engineering, Kinshasa, Democratic Republic of the Congo

Correspondence: Anthony Bassesuka Sandoka Nzao, ISTA Kinshasa, Electrical Engineering, Kinshasa, Democratic Republic of the Congo. E-mail: bass_sandoka@yahoo.fr

Received: March 8, 2024 Accepted: June 19, 2024 Online Published: July 19, 2024

doi:10.5539/cis.v17n2p7 URL: https://doi.org/10.5539/cis.v17n2p7

Abstract

The coexistence of electronic power and control systems in the same box presents a serious threat to the proper functioning of electronic systems integrated into automobiles, aeronautics and space. Thus, managing the electromagnetic compatibility of these systems constitutes a challenge, particularly given electromagnetic phenomena. This paper describes a simulation study and application of the partial element equivalent circuit method to model the prediction of radiated emissions from the onboard electronic cable system. In this article, we first explain the use of the partial cell equivalent circuit modeling method, then describe its mathematical formulation and introduce the different electromagnetic phenomena it considers in connection with wiring, then propose radiation calculations electromagnetic as a function of the geometry of the discrete cells taking into account the increase in frequency. The goal is to get as close to the structure as possible. To balance the accuracy and speed of the proposed method, we replaced the partial capacities with the equivalent capacities so as to considerably minimize the number of capacities, the complexity of the system and the computational time requirement. This option adapts the partial element equivalent circuit method to the study of larger structures such as cable structures and provides an efficient and rapid way to simulate electromagnetic radiation. To achieve this objective, we have associated the physical laws of electromagnetic wave propagation with the method of modeling equivalent circuits using partial elements because it is easy to manipulate flat surfaces and cables. 2D simulations based on the proposed models were developed as well as the verification of the consistency of the different models, by comparing the fractal dimensions of the program results with those of the figures obtained experimentally.

Keywords: study, modeling, radiated em emissions, partial element equivalent method, maxwell's equations, 2D simulation, embedded electronic wiring systems, physical laws, electromagnetic interference

1. Introduction

The share of electronics in embedded systems (automobile, aeronautics, space, etc.) continues to grow. Supported by its strong integration, this electronics provides greater performance and makes it possible to offer solutions to meet requirements, such as safety and comfort. However such rapid development requires taking into account any marginal phenomenon that could harm the proper functioning of electronic systems (Amadou Bayaghiou DIALLO, 2023), (European Directive, 1989), (M. Toure, 2019), (F. A. Kharanaq, A. Emadi, and B. Bilgin, 2020), (K. Kadem, 2020) and (Y. J. Hwang and J. Y. Jang, 2020). In the same way as thermal management or the management of mechanical constraints, electromagnetic interference has become a risk phenomenon of very great importance for any signal or power electronics system. We are then talking about a concern for electromagnetic compatibility (EMC) with which manufacturers find themselves confronted (European Directive, 2004), and (Y. J. Hwang and J. Y. Jang, 2020).

The use of high frequency (HF) components can have a multi-component effect that increases the electron density in the vacuum of the system, which is likely to result in degradation of hardware performance and damage to system components and components render them partially or even completely unusable (Nicolas Fil, 2017).

The growing number of static conversion devices (power electronics) in the automotive industry and their

increasingly significant impact on vehicle electronics and the vehicle's electrical network impose ever stricter limits in terms of reliability and safety. (Amadou Bayaghiou DIALLO, 2023), (M. Touré, 2019)) and (F. A. Kharanaq, A. Emadi and B. Bilgin, 2020). The effects of the disturbances listed on electronic circuits strongly depend on the type of circuit, that is to say, its digital or analogue nature (Barber et al, 1994), (Tristan Dubois, 2009). Switching phenomena, interference and electromagnetic risks are becoming central in embedded electronic architectures. The limited appearance of different types of electrical circuits for energy, mobility, control and information transmission of the embedded system induces a new, very difficult internal and external electromagnetic environment. (Jean-Marc Dienot, 2010). Today, applications of communication and image have taken on significant importance on a global level. These civil or military applications must present proven functional safety in all areas, including that of electromagnetism (K. Kadem, M. Bensetti, Y. Le Bihan, E. Travail and M. Femmes, 2021) and (Mersha and C. From, 2022). However, the electromagnetic sensitivity threshold of complex electronic circuits at the heart of these systems is reduced (Tristan Dubois, 2009), (Ramdani and al, 2009). This increased vulnerability is due to the decrease in their size, their supply voltage and the increase in their operating frequency (V. Varvolik, D. Prystupa, G. Buticchi, S. Peresada, M. Galea and S. Bozhko, 2021) and (L. Di Leonardo, M. Popescu, M. Tursini and M. Villani, 2019).

To estimate the level of EM pollution caused by sources of interference such as static converters, the use of measurement initially seemed the most natural solution (Amadou Bayaghiou DIALLO, 2023). Unfortunately, this approach is no longer sufficient because it leads to considering EMC too late in the system design cycle (L. Di Leonardo, M. Popescu, M. Tursini and M. Villani, 2019ja (W. Wang. Fang, H. Cui, F. Li, Y. Liu and T.J. Goodbye, 2022). Furthermore, standard EMC measurements at the individual device level do not necessarily guarantee an acceptable overall level, because the implementation of a series of devices is much more complex than for individual devices. Furthermore, electromagnetic compatibility measurements may not be repeated, the number of parameters to be measured can be very large and the costs of an EMC measurement campaign are often prohibitive (K. Kadem, 2020) yes (Y. J. Hwang Kaj., J. Y. Jang, 2020).

From the above and according to European standards, EMC is the ability of a system to operate in its EM environment satisfactorily and without itself producing intolerable EM disturbances for the equipment in its environment. Therefore, the EMC participates in the design and integration of electronics. For the study of EMC to be valid, it must be able to treat and resolve these two main aspects (M. Toure, 2019), (F. A. Kharanaq, A. Emadi, and B. Bilgin, 2020), (K. Kadem, 2020) and (Y. J. Hwang and J. Y. Jang, 2020):

- Emission: Systems must not emit annoying EM disturbances into their EM environment.

- Immunity: systems must be able to operate in their EM environment.

We must therefore note that in automobiles, the classic term to designate these two aspects of EMC are respectively: muteness (for emission) and susceptibility (for immunity).

In recent decades, the evolution of electronic equipment and the proliferation of cable networks as a means of transport have favoured the increase in electromagnetic incompatibility phenomena. In other words, it has been observed that the cohabitation of this equipment in the same environment creates malfunctions; new sources of unintentional emission of electromagnetic waves are thus caused. There are also other sources of disruption. As a result, the evaluation of electromagnetic coupling thresholds within these electrical installations has become essential to anticipate critical situations generating internal malfunctions and remedy them (Aymene Chafik, 2019), (O. W. Henry, 2009).

To limit the risk of EM interference with other devices and in particular with control devices, it is necessary to first predict the EM emissions generated and then limit the disturbances harmful to the operation and safety of the system overall. Therefore, it is important to predict the conducted and radiated emissions of cables which are, by their large size, a potential EM risk for the surrounding electronic system by advocating the need to separate the power cables from the control cables.

According to (Acharf Liakouti, 2017) the use of electrical cables as a digital data transmission medium in applications such as Internet access or home automation is certainly very attractive. However, unintended electromagnetic radiation generated by wired systems can be a source of EM interference and create a bothersome electromagnetic compatibility (EMC) problem. The evaluation of this near-field radiation is therefore of capital importance.

We can also do EMC filtering which is an interesting and more popular solution in the embedded electronic system industry.

We must remember that depending on the mode of propagation of EM disturbances, there are two types of

impedances to consider, depending on numerous parameters of the embedded electronic system, which can create disturbances such as the topology, the parasitic elements of the components and the layout geometry of cabling which are also proposed solutions.

To circumvent the risk of EM interference with other equipment and in particular control equipment, it is first necessary to predict the radiated EM emissions likely to interfere with the operation and safety of the entire system. It is therefore necessary to predict emissions from cables which, due to their large dimensions, represent a possible EM risk for surrounding electronic systems.

To balance the accuracy and speed of the proposed method, the equivalent capacities replace the large number of partial capacities. In this way, we significantly reduce the number of capacities and reduce system complexity. This makes the PEEC method better suited to the study of larger structures such as cabling structures, reduces the computational time requirement and provides an efficient and fast radiated EM emissions simulation tool.

Apart from the results obtained by the 2D simulations based on the proposed models, we proceeded to verify the consistency of the different models, by comparing the fractal dimensions of the results of our programs with those of the figures obtained experimentally, in order to implement the physical laws of electromagnetic wave propagation (Maxwell's equations) associated with the PEEC (Partial Element Equivalent Circuit) modeling method given its ease of treating flat surfaces in the same way as cables.

2. Theoretical Models

2.1 EM Modeling Associated With the PEEC Method

EM modeling methods are based on the four Maxwell equations described below.

Differential formulation :	Full formulation :
$\nabla \times \vec{H} = \vec{J} + \frac{\partial \vec{D}}{\partial t}$	$\oint_C \vec{H} \cdot d\vec{l} = I + \int_S \frac{\partial \vec{D}}{\partial t} \cdot d\vec{S}$
$\nabla \times \vec{E} = -\frac{\partial \vec{B}}{\partial t}$	$\oint_C \vec{E} \cdot d\vec{l} = -\int_S \frac{\partial \vec{B}}{\partial t} \cdot d\vec{S}$
$\nabla \cdot \vec{H} = 0$	$\oint_S \vec{B} \cdot d\vec{S} = 0$
$\nabla \cdot \vec{D} = \rho$	$\oint_S \vec{D} \cdot d\vec{S} = Q$

In Maxwell's equations, Q is the electric charge, $\vec{B}$ is the magnetic induction, $\vec{D}$ is the electric induction, $\vec{E}$ is the electric field, $\vec{H}$ is the magnetic field, $\vec{j}$ is the current density, t is the time and ρ is the volume charge (A. Ruehli, 1974). These Maxwell equations are not sufficient to solve an electromagnetic problem and do not make it possible to determine the unknowns $\vec{E}(\vec{r},t)$, $\vec{H}(\vec{r},t)$, $\vec{B}(\vec{r},t)$, and $\vec{D}(\vec{r},t)$ to the extent that each of these variables is a vector of 3 components (Constantine., and A. Balanis, 1996). So, we obtain more unknowns than equations. To overcome this difficulty, additional hypotheses linking the different unknowns are necessary (Roger F., and Harrington, 2015): these are the constitutive relations ((1), (2) and (3)). They take into account the permittivity, permeability and conductivity of the continuous medium considered. For this species, the medium between conductors is air, the permittivity and permeability of which are given respectively by ε_0 and μ_0 (J. L. Volakis., A. Chatterjee., and L. C. Kempel, 1998). In addition, we will use copper as a conductor whose conductivity is given by par $\sigma = 59{,}6 * 10^6 \mathrm{m.S}^{-1}$ (M.N.O. Sadiku., 1994).

$$\vec{J} = \sigma * \vec{E} \quad (1)$$

$$\vec{B} = \mu_0 * \vec{H} \quad (2)$$

$$\vec{D} = \varepsilon_0 * \vec{E} \quad (3)$$

The mathematical formulation of the PEEC method was mainly developed by (Constantine A. Balanis; 1996), (J. L. Volakis., A. Chatterjee., and L. C. Kempel, 1998) and (A. Ruehli, 1974). According to the electric field integral equation, a time t and a point $\vec{r}$, the total electric field $\vec{E}^T$ is the sum of the incident field $\vec{E}^i$ and the self-induced field $\vec{E}$ (Yu Zhu, 2006).

$$\vec{E}^T(\vec{r},t) = \vec{E}^i(\vec{r},t) + \vec{E}(\vec{r},t) \quad (4)$$

When the point $\vec{r}$, belongs to a conductor, the total electric field is given by the following relation:

$$\vec{E}^{T}(\vec{r},t) = \frac{\vec{J}(\vec{r},t)}{\sigma} \quad (5)$$

whose electrical conductivity is σ. In the previous relation, the incident field $\vec{E}^{i}(\vec{r},t)$ only depends on sources external to the system. It is therefore independent of the currents and charges present at point $\vec{r}$, of the structure, unlike the induced field which is a result of these. Indeed, the induced electric field is written (Wenns Yannick; 2006) and (Wissem Yahyaoui; 2012):

$$\vec{E}(\vec{r},t) = -\frac{\delta\vec{A}(\vec{r},t)}{\delta t} - \nabla\varphi(\vec{r},t) \quad (6)$$

Where $\vec{A}$ is the vector potential and φ is the scalar potential.

$$\vec{A}(\vec{r},t) = \mu_0 \int_{v'} \vec{G}(\vec{r},\vec{r}').\vec{J}(\vec{r}',t_d).dv' \quad (7)$$

$$\varphi(\vec{r},t) = \frac{1}{\varepsilon_0}\int_{S'} \vec{G}(\vec{r},\vec{r}').\sigma_S(\vec{r}',t_d).dS' \quad (8)$$

In relation (8), σ_s is the surface density of the electric charges which are physically present on the surface of the conductors and t_d is the delay time between the source and the observation point $\vec{r}$. This time is given by : $t_d = t - |\vec{r} - \vec{r}'|/c$, with c the celerity of the vacuum (I. Yahi., F. Duval., and A. Louis, 2007) and (I. Yahi, 2009).

In equations (7) and (8), G is called Green's function and is given by:

$$\vec{G}(\vec{r},\vec{r}') = \frac{1}{4\pi}\frac{1}{|\vec{r}-\vec{r}'|} \quad (9)$$

Using the relations (5) and (6), the incident field becomes:

$$\vec{E}^{i}(\vec{r},t) = \frac{\vec{J}(\vec{r},t)}{\sigma} + \frac{\delta\vec{A}(\vec{r},t)}{\delta t} + \nabla\varphi(\vec{r},t) \quad (10)$$

To transform relation (10) into an electric field integral equation (EFIE), the definition of the electromagnetic potentials $\vec{A}$ and φ can be used. This allows us to have the following relationship:

$$\vec{E}^{i}(\vec{r},t) = \frac{\vec{J}(\vec{r},t)}{\sigma} + \mu_0 \int_{v'} \vec{G}(\vec{r},\vec{r}').\frac{\delta\vec{J}(\vec{r}',t_d)}{\delta t}.dv' + \frac{\nabla}{\varepsilon_0}\int_{S'} \vec{G}(\vec{r},\vec{r}').\sigma_S(\vec{r}',t_d).dS' \quad (11)$$

The presentation of equation (11) in a Cartesian frame of reference allows us to have tree scalar equations, each of which corresponds to an axis. In the absence of an incident electric field, these equations are summarized in the relation (12) in which *γ = x, y* or *z*.

$$\vec{E}^{i}{}_{\gamma}(\vec{r},t) + \mu_0 \int_{v'} \vec{G}(\vec{r},\vec{r}').\frac{\delta\vec{J}(\vec{r}',t_d)}{\delta t}.dv' + \frac{1}{\varepsilon_0}\frac{\partial}{\partial\gamma}\left(\int_{S'} \vec{G}(\vec{r},\vec{r}').\sigma_S(\vec{r}',t_d).dS'\right) = 0 \quad (12)$$

A discretization of the structure into N_v volume cells and N_s surfaces makes it possible to obtain the charge density and the current density in the form of a linear combination defining what is called the Petrov-Galerkin approach. The densities are written as in the following two relationships:

$$\vec{J}(\vec{r},t) = \sum_{m=1}^{N_s} \vec{j}_m(t_{dm}) f_m(\vec{r}) \quad (13)$$

$$\sigma(\vec{r},t) = \sum_{n=1}^{N_s} \sigma_n(t_{dn}) g_n(\vec{r}) \quad (14)$$

With $f_m(\vec{r}) = 1$ when the point $\vec{r}$ belongs to the volume v_m and $f_m(\vec{r}) = 0$ elsewhere. Likewise, $g_n(\vec{r}) = 1$ when $\vec{r}$ belongs to the surface s_n et $g_n(\vec{r}) = 0$ elsewhere. The volumes and elementary cells are quite small. This ensures that the current and the charge are constant. $t_{dm} = t - |\vec{r} - \vec{r}_m|/c$ and $t_{dn} = t - |\vec{r} - \vec{r}_n|/c$ respectively represent the delay times between the volume cell v_m and the surface S_n with respect to the point $\vec{r}$.

The level of each volume cell, the current density is given by the ratio between the current $I_{\gamma m}$ and the section of the cell a_m.

$$J_{\gamma m}(t_{dm}) = \frac{I_{\gamma m}(t_{dm})}{a_m} \quad (15)$$

Also, the charge density defined at the level of each elementary surface is written as a function of the quantity of surface charges :

$$\sigma_{Sn}(t_{dn}) = \frac{Q_n^T(t_{dn})}{S_n} \tag{16}$$

The association of equations (15) and (16) with equations (13) and (14) allows us to have the respective current and charge densities as a function of the currents and the quantities of charges:

$$\vec{\mathrm{J}}(\vec{\mathrm{r}},\mathrm{t}) = \sum_{\mathrm{m}=1}^{\mathrm{N_s}} \frac{I_{\gamma m}(\mathrm{t_{dm}})}{a_m}\ f_m(\vec{\mathrm{r}}) \tag{17}$$

$$\sigma_S(\vec{\mathrm{r}},\mathrm{t}) = \sum_{\mathrm{n}=1}^{\mathrm{N_s}} \frac{Q_n^T(t_{dn})}{S_n}\mathrm{g_n}\,(\vec{\mathrm{r}}) \tag{18}$$

From the discretization ((13) to (18)), it becomes possible to present the EFIE equation, defined by relation (12), in the form of an equation interpretable in an RLC equivalent circuit. Indeed, by substituting relations (17) and (18) into equation (12), we obtain:

$$\vec{E}_{\gamma}(\vec{\mathrm{r}},\mathrm{t}) + \sum_{\mathrm{m}=1}^{\mathrm{N_s}} \frac{\mu_0}{a_m}\int_{\mathrm{Vm'}} \vec{\mathrm{G}}(\vec{\mathrm{r}},\vec{\mathrm{r}}'_m)\frac{\partial I_{\gamma m}(\mathrm{t_{dm}})}{\partial t}\mathrm{d}v_m + \sum_{\mathrm{n}=1}^{\mathrm{N_s}} \frac{1}{a_n\varepsilon_0}\frac{\partial}{\partial\gamma}\left(\int_{S_n} \vec{\mathrm{G}}(\vec{\mathrm{r}},\vec{r}_n).\frac{Q_n^T(t_{dn})}{S_n}ds\right) = 0 \tag{19}$$

This relation is valid for any point $\vec{r}$, whether it belongs to the structure or not. We choose $\vec{r} = \vec{r}_i$ a point belonging to the discretization volume v_i of the structure. Figure 1 below gives the structure taking into account the capacitive effect (Wissem Yahyaoui, 2012) and (J. Ekman., and G. Antonini, 2004).

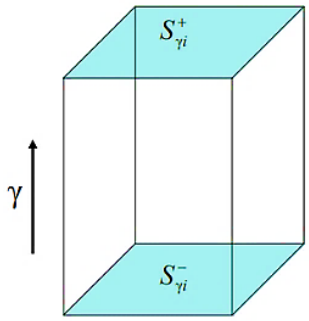

Figure 1. Surfaces for calculating the capacitive effect (Wissem Yahyaoui; 2012) and (J. Ekman., and G. Antonini, 2004)

The relationship remains valid. By integrating each of the members of the equation by the operator defined by the relation (20) and by applying the fundamental theorem of integral calculus (21) to the 3rd term of the equation, we obtain the relation (22) in which $S_{\gamma i}^{+}$ and $S_{\gamma i}^{-}$ in Figure 1 above are two surfaces highlighting the capacitive aspect (A. Müsing., J. Ekman., and J.W. Kolar, 2009).

$$\frac{1}{a_{\gamma i}}\int_{v_i} dv_i = \frac{1}{a_{\gamma i}}\int_{v_i} dS_i d\gamma \tag{20}$$

$$\int_v \frac{\partial}{\partial\gamma}F(\gamma)\,dv = \int_{S_{\gamma^+}} F(\gamma^+)\,dS_{\gamma^+} - \int_{S_{\gamma^+}} F(\gamma^-)\,dS_{\gamma^-} \tag{21}$$

$$\frac{1}{a_{\gamma i}} + \sum_{\mathrm{m}=1}^{\mathrm{N_s}} \frac{\mu_0}{a_m.a_{\gamma i}}\int_{v_i}\int_{\mathrm{Vm'}} \vec{\mathrm{G}}(\vec{\mathrm{r}},\vec{\mathrm{r}}'_m)\frac{\partial I_{\gamma m}(\mathrm{t_{dmi}})}{\partial t}\mathrm{d}v_m.dv_i + \sum_{\mathrm{n}=1}^{\mathrm{N_s}} \frac{1}{a_n\varepsilon_0 a_{\gamma i}}\left(\left(\int_{S_n}\int_{S_{\gamma^+}} \vec{\mathrm{G}}(\vec{\mathrm{r}},\vec{r}_{ni})\,Q_n^T(t_{dn}).ds.dS_i\right) - \frac{1}{a_n\varepsilon_0 a_{\gamma i}}\left(\int_{S_n}\int_{S_{\gamma^-}} \vec{\mathrm{G}}(\vec{\mathrm{r}},\vec{r}_n)\,Q_n^T(t_{dni}).dS\right)\right) \tag{22}$$

Equation (22) constitutes the beam of the PEEC method. It allows the deduction of different partial elements. However, adequate discretization is necessary to arrive at the global equivalent circuit. This equation allows the deduction of an equivalent electrical circuit from Figure 2 below, the calculations of the partial elements of which are proposed in the literature of (Wissem Yahyaoui, 2012), (E.Vialardi, 2003), (F. Duval, 2007), (C. Ho., A. Ruehli., and P. Brennan, 1975) and (G. Antonini., J. Ekman., and A. Orlandi, 2003).

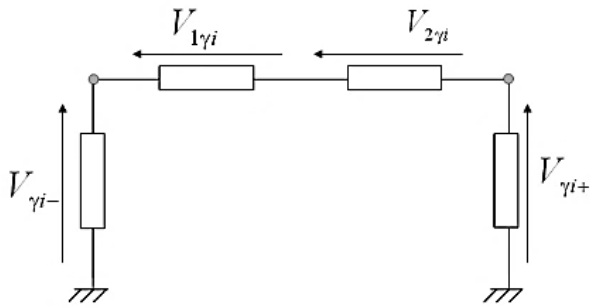

Figure 2. Circuit equivalent to a generic volume cell (Wissem Yahyaoui; 2012) and (G. Antonini., and A. Ruehli, 2003), (Mr. Besacier, 2001) and (Tran Thanh Son, 2008)

To analyze and compare the results obtained in the simulation, we go through the following points :

2.2 Electromagnetic Model of On-board Electronic Wiring System

The transition from the electric field integral equation (EFIE) to the PEEC method is done by discretizing the conductors into volumes and surfaces that can be used to obtain the RLC equivalent circuit (J. Ekman, 2003), (J. Ekman., and Lundgren Urban, 2001) and (G. Antonini., J. Ekman., and A. Orlandi, 2003). The choice of the dimensions of the discretization cells, whether volumetric or surface, is directly linked to the maximum working frequency, the desired calculation precision and therefore the calculation time (J. Ekman, 2003) and (S. Mei and Y. Ismail, 2003).

According to the work proposed by (E.Vialardi, 2003) for the integration of the capacitive effect in the EM PEEC model, we can use two different circuit-type models:

- A model associating in series a pseudo-capacitance and a voltage generator controlled in voltage (Wissem Yahyaoui, 2012), (E.Vialardi, 2003), (F. Duval, 2007), this controlled source is controlled by all the tensions of the other elements of the mesh;

- A model comprising in parallel a pseudo-capacitor and a current generator controlled by current (Wissem Yahyaoui, 2012).

The generator is also controlled by all elements of the mesh. Unlike the inductive calculation which is only done in the same direction as the current, the capacitive calculation is done for parallel cells as well as for perpendicular cells (E.Vialardi, 2003) and (A. E. Ruehli., G. Antonini., and A. Orlandi, 1999).

This necessarily leads to a very large number of calculations for large structures. However, the trickiest part is extracting an equivalent electrical circuit. Indeed, the concept of a controlled source makes all the cells interact, and when the number of them is large, it becomes difficult to implement this type of assembly, adding to this the possible limitations linked to the electrical simulation software used (Wissem Yahyaoui, 2012), (E.Vialardi, 2003) and (F. Duval, 2007). The capacitive coupling in the PEEC method is calculated between each pair of cells of the system discretized in three dimensions. The finer the discretization, the heavier the calculation becomes (Wissem Yahyaoui, 2012).

To obtain a wiring model taking into account the effects cited above and considering the discretization procedure proposed in the literature of (Martin Ludwig Zitzmann, 2007) and (Kenneth and L. Kaiser, 2004), in the framework of this article, we implement the model in Figure 3 below to describe the behaviour, both electrical and electromagnetic, of the entire structure (T. V. Dinh., B. Cabon., and J. Chilo, 1990).

To obtain a wiring model taking into account the effects cited above and considering the discretization procedure proposed in the literature of (Martin Ludwig Zitzmann, 2007) and (Kenneth., and L. Kaiser, 2004), in the framework of this article, we implement the model in Figure 3 below to describe the behaviour, both electrical and electromagnetic, of the entire structure (A. Ruehli., and H. Heeb, 1992) and Sergey V. Kochetov. (2008).

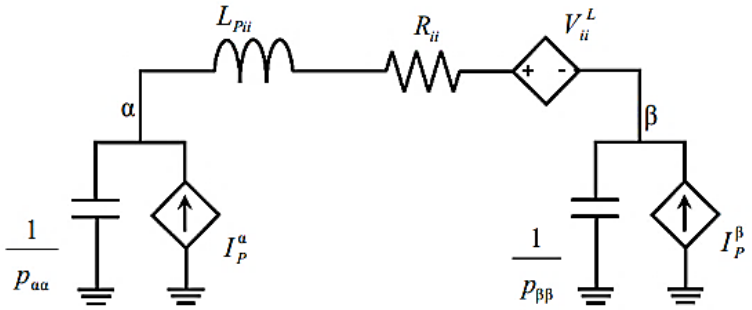

Figure 3. Equivalent circuit of a discretization cell (Martin Ludwig Zitzmann; 2007), (E. Clavel, 1996) and (Kenneth L. Kaiser; 2004).

2.3 Cable Electromagnetic Parameters Models

The circuit equivalent to a discretization cell which is placed between two nodes is made up of three partial elements (Y. Ji and T. Hubing, 2000). First, the partial inductance specific to each volume cell as well as the mutual partial inductances between them. These elements represent the magnetic coupling in the equivalent circuit (G. Wollenberg., and S. V. Kochetov, 2003). The second element, which presents the capacitive effect, is the potential coefficient representing the electrical coupling between the surfaces which surround each of the nodes. Finally, the third element of the equivalent circuit is its resistance (Martin Ludwig Zitzmann, 2007), (C.-S. Yen., Z. Fazarinc., and R. L. Wheeler, 1982) and (Kenneth., and L. Kaiser, 2004).

By applying Ohm's law in the circuit of Figure 2, we obtain the following relationship (G. Antonini., A. E. Ruehli., J. Esch., J. Ekman., A. Mayo., and A. Orlandi, 2003):

$$V_{1\gamma i} = \frac{1}{a_{\gamma i}} \iiint_{V_i} \frac{J_\gamma(\vec{r}_i,t)}{\sigma_{\gamma i}} dV_i \tag{23}$$

The current density J_γ is uniform in the same discretization cell. This allows us to write:

$$V_{1\gamma i} = \frac{1}{a_{\gamma i}} \frac{J_\gamma(t)}{\sigma_{\gamma i}} v_i = \frac{1}{a_{\gamma i}} \frac{l_{\gamma i}}{\sigma_{\gamma i}} I_\gamma(t) \tag{24}$$

Thus, we determine the first element of the equivalent circuit of a cell which is the resistance. The latter is given by (Cyril Buttay, 2004) :

$$R_{ii} = \frac{1}{a_{\gamma i}} \frac{l_{\gamma i}}{\sigma_{\gamma i}} \tag{25}$$

Where $a_{\gamma i}$ represents the cell volume section, γ is the direction of the current and $l_{\gamma i}$ is the length of the cell in the direction of the current. Furthermore, $a_{\gamma i}$ is the cross-sectional area of the cell (i). Furthermore, considering the inductive effect, the voltage $V_{2\gamma i}$ in Figure 2 is defined in the form of the equation (Y. Ji., and T. Hubing, 2000) and (J. Garrett., A. E. Ruehli., and C. R. Paul, 1998):

$$V_{2\gamma i} = L_{pii} \frac{\partial I_{\gamma m}(t)}{\partial t} + V_{ii}^{L} \tag{26}$$

Where the voltage V_{ii}^{L} is that induced by the other discretization cells. It is written:

$$V_{ii}^{L} = \sum_{\substack{J=1 \\ i \neq J}}^{N_v} L_{pii} \frac{\partial I_{\gamma j}(t_{dji})}{\partial t} \tag{27}$$

The mutual partial inductance is given by the following, the calculation details of which are described in (E.Vialardi, 2003), (E. Clavel, 1996), (A. E. Ruehli, 1972) and (F. Duval, 2007) :

$$L_{pij} = \frac{\mu_0}{4\pi a_i a_j} \iiint_{V_i} \left(\iiint_{V_j} \frac{1}{|\vec{r}_i - \vec{r}_j|} dV_i \right) dV_i \tag{28}$$

Starting from the model in Figure 4 at node α, the circuit equivalent to the capacitive effect is determined as shown in Figure 4 below (Y. Ji and T. Hubing, 2000).

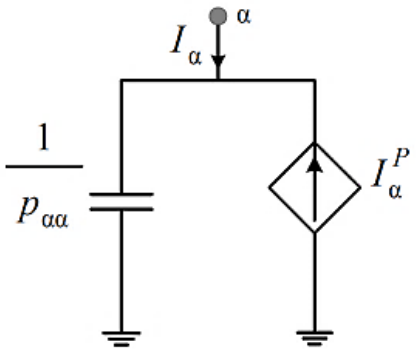

Figure 4. Circuit equivalent to the capacitive effect (K. M Coperich., A. E. Ruehli., and A. Cangellaris, 2000)

By consideration of the capacitive effect, the voltage at the node (α) in Figure 4 is given by the following relationship :

$$V_\alpha(t) = \sum_{\substack{J=1 \\ \beta=1}}^{N_s} p_{\alpha\beta}\, Q_\beta^T(t_{d_{\alpha\beta}}) \tag{29}$$

Considering the temporal variation of the $V_\alpha(t)$ and, and dividing $\frac{1}{p_{\alpha\alpha}}$, we obtain the relation :

$$\frac{1}{p_{\alpha\alpha}} \frac{\partial V_\alpha(t)}{\partial t} = I_\alpha(t) + I_\alpha^P(t) \tag{30}$$

Furthermore, the component $I_\alpha^P(t)$ is calculated as follows :

$$I_\alpha^P(t) = \sum_{\substack{J=1 \\ \beta=1 \\ \beta\neq\alpha}}^{N_s} \frac{p_{\alpha\beta}}{p_{\alpha\alpha}} I_\beta(t_{d_{\alpha\beta}}) \tag{31}$$

To model the capacitive effect, it is sufficient to determine the potential coefficient between two nodes (α) and (β) of the model in Figure 3. This potential coefficient is defined by the Maxwell-Gauss theorem. The analytical expression of the potential coefficient is determined according to two cases: parallel surfaces and perpendicular surfaces were developed and presented in (Wissem Yahyaoui, 2012), (Y. Ji and T. Hubing, 2000), (Martin Ludwig Zitzmann, 2007) and (Kenneth and L. Kaiser; 2004).

$$p_{\alpha\beta} = \frac{1}{4\pi\varepsilon_0 S_\alpha S_\beta} \oiint_{S_\alpha} \left(\oiint_{S_\beta} \frac{1}{|\vec{r}_\alpha - \vec{r}_\beta|} dS_\alpha \right) S_\beta \tag{32}$$

A node is surrounded by more than a single surface. In the case of a square section cable, four external surfaces are defined around each node.

Considering (α) and (β) two nodes of Figure 3 to which we associate the total surfaces S_α And S_β. Each surface can be subdivided into 4 exterior surfaces. S_α and S_β are respectively the union of S_{il} And S_{jk}. It is therefore possible to write the following relation (A. E. Ruehli., and P. A. Brennan, 1973):

$$\oint_{S_\alpha} \oint_{S_\beta} \frac{1}{|\vec{r}_\beta - \vec{r}_\alpha|} dS_\alpha\, dS_\beta = \sum_{k=1}^{4} \sum_{m=1}^{4} \oint_{S_{\beta_k}} \oint_{S_{\alpha_l}} \frac{1}{|\vec{r}_{\beta_k} - \vec{r}_{\alpha_l}|} dS_{\alpha_l} dS_{\beta_k} \tag{34}$$

Thus, the potential coefficient is generally written in the form:

$$p_{\alpha\beta} = \frac{1}{4\pi\varepsilon_0 S_\alpha S_\beta} \sum_{k=1}^{4} \sum_{l=1}^{4} \oint_{S_{\beta_k}} \oint_{S_{\alpha_l}} \frac{1}{|\vec{r}_{\beta_k} - \vec{r}_{\alpha_l}|} dS_{\beta_k} dS_{\alpha_l} \tag{35}$$

The work proposed in the literature by (G. Antonini., A. E. Ruehli., J. Esch., J. Ekman., A. Mayo., and A. Orlandi, 2003), shows that from this equation we deduce the need for weighting in the calculation of the 3D potential coefficient. For this purpose, the final potential coefficient is obtained through the relation (36) below. It is necessary to remember that the resolution of a complete system containing these potential coefficients, leads to the definition of the matrix of potential coefficients, each element of which is calculated according to the case defined by equation (36).

$$p_{\alpha\beta} = \frac{1}{4\pi\varepsilon_0 S_\alpha S_\beta} \sum_{k=1}^{4}\sum_{l=1}^{4} \oint_{S_{\beta_k}} \oint_{S_{\alpha_l}} \frac{1}{\left|\vec{r}_{\beta_k} - \vec{r}_{\alpha_l}\right|} dS_{\beta_k} dS_{\alpha_l} = \sum_{k=1}^{4}\sum_{l=1}^{4} \frac{S_{\beta_k} S_{\alpha_l}}{S_\alpha S_\beta} p_{\alpha_l \beta_k} \quad (36)$$

This technique is all the more precise as these two conditions are satisfied: the surfaces surrounding the nodes are equipotential and also admit the same charge density (J. Ekman and S. Niska, 2004). When the working frequency increases and it becomes necessary to discretize a wiring structure as finely as possible, the number of surface cells becomes enormous and the systems are complex to solve (Wissem Yahyaoui, 2012). Indeed, the matrix of potential coefficients is a full matrix whose dimension increases very quickly as a function of discretization (G. Antonini., A. E. Ruehli., J. Esch., J. Ekman., A. Mayo., and A. Orlandi, 2003) and (Wissem Yahyaoui ; 2012). And, inverting a system containing such a matrix requires more calculation time and memory. For this, it was necessary to consider a new capacitive calculation proposed in the work of (J. Ekman, 2003) and (J. Ekman, 2003).

In order to solve this EM problem modeled for Figure 3, two possibilities present themselves (H.A. Wheeler, 1942) and (C.-S. Yen., Z. Fazarinc., and R.L. Wheeler, 1982). The first is based on the creation of a circuit-type file processable by a SPICE-type simulator (TV Dinh., B. Cabon., and J. Chilo, 1990) and (G. Wollenberg and S.V. Kocheto, 2003). In this circuit file, we define the circuit elements which are the inductances, the resistances, the inductive couplings, the own partial capacitance and the sources controlled by current presenting the capacitive couplings (Mathias Enohnyaket, 2008), (V. Ardon., O. Chadebec., JM. Guichon., and E. Vialardi, 2008) and (Vincent Ardon., Jérémie Aimé, Olivier Chadebec., Edith Clavel., and Enrico Vialardi, 2009). The second type of resolution uses matrix inversion. This resolution is mathematically equivalent to that of circuit type (J. Ekman and S. Niska, 2004). Its advantage is that it is not limited to the number of circuit elements as is the case with certain circuit simulation tools (S. Mei and Y. Ismail; 2003), (S. Mei and Y. Ismail; 2004), (M. Enohnyaket ; 2007) and (M. Enohnyaket and J. Ekman ; 2009).

2.4 Modeling Radiated Emissions

The modeling of the contribution in radiated emissions from each discretization cell takes into account the currents in the structure, obtained by the PEEC method. Firstly, a discretization cell is considered equivalent to a dipole. So, in this case, only one dimension, which is the length, is considered. To achieve this goal, two main approaches can be used for such a calculation: the quasi-steady state approximation and the infinitesimally small dipole approximation (Y. Ji and T. Hubing, 2000).

Starting from the wave equations are obtained from the Maxwell equations described previously. For the electric and magnetic fields in which we are interested, the wave equations, a point $\vec{r}$ and at time t, are given respectively by (M. W. Ali., T. H. Hubing., and J. L. Drewniak. (1997) :

$$\vec{\nabla} \times \vec{\nabla} \times \vec{E}(\vec{r}, t) + \mu_0 \varepsilon_0 \frac{\partial^2}{\partial t^2} \vec{E}(\vec{r}, t) = \mu_0 \frac{\partial^2}{\partial t^2} \vec{J}(\vec{r}, t) \quad (37)$$

$$\vec{\nabla} \times \vec{\nabla} \times \vec{H}(\vec{r}, t) + \mu_0 \varepsilon_0 \frac{\partial^2}{\partial t^2} \vec{H}(\vec{r}, t) = \mu_0 \nabla \times \vec{J}(\vec{r}, t) \quad (38)$$

Where $\vec{E}$ is the electric field, $\vec{H}$ is the magnetic field and μ_0 and ε_0 are the magnetic permeability and electric permittivity of air (vacuum), respectively. The wave equations are written as follows (T. Hubing, 1991) :

$$\Delta \vec{E}(\vec{r}, t) - \mu_0 \varepsilon_0 \frac{\partial^2}{\partial t^2} \vec{E}(\vec{r}, t) = \frac{1}{\varepsilon_0} \nabla \rho(\vec{r}, t) + \mu_0 \frac{\partial}{\partial t} \vec{J}(\vec{r}, t) \quad (39)$$

$$\vec{\nabla} \times \vec{\nabla} \times \vec{H}(\vec{r}, t) + \mu_0 \varepsilon_0 \frac{\partial^2}{\partial t^2} \vec{H}(\vec{r}, t) = \nabla \times \vec{J}(\vec{r}, t) \quad (40)$$

We know that the fields $\vec{E}(\vec{r}, t)$ and $\vec{H}(\vec{r}, t)$ can be written in terms of the vector potential $\vec{A}$ and the scalar potential $\vec{A}$. The notion of potentials was used to simplify the resolution of Maxwell's equations. Figure 5 below shows the structure of a discretized cell (Jack Vanderlinde, 2005).

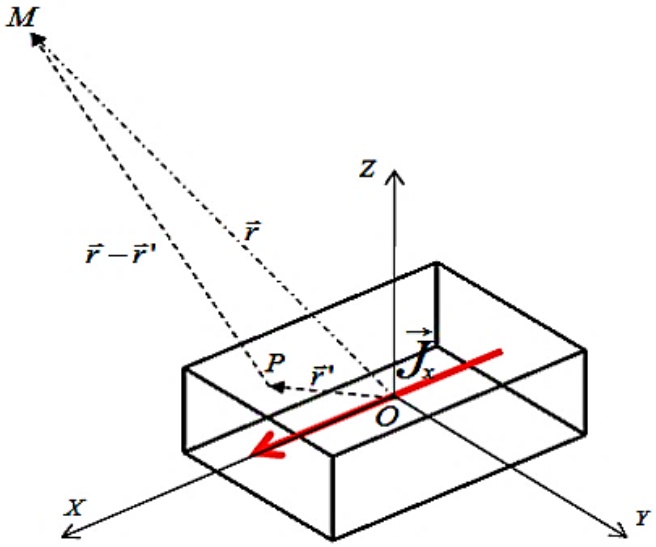

Figure 5. Discretization cell

We demonstrate that, for a cell crossed by a current and whose section is very small compared to the length, the radiation will be considered equivalent to that generated by an electric dipole. Thus, the vector potential is given by (J. Jin., And J. Douglas, 2009) :

$$\vec{A} = \frac{\mu_0}{4\pi} I \int_c \frac{e^{-jk|\vec{r}-\vec{r'}|}}{|\vec{r}-\vec{r'}|} d\vec{l'} \tag{41}$$

Where I is the current passing through the cell and C is the length.

The radiated emissions are perfectly defined by the magnetic field and the electric field. Using the Lorentz gauge, we can write the electric field as a function of the vector potential alone (Jean-Paul Gonnet, 2005).

$$\vec{H} = \frac{1}{\mu_0}\vec{\nabla} \times \vec{A} \qquad = \tag{42}$$

$$\vec{E} = \frac{1}{j\omega\varepsilon_0\mu_0}\vec{\nabla} \times \vec{\nabla} \times \vec{A} \tag{43}$$

We consider the discretization cell presented in Figure 5. The vector potential is given by:

$$\vec{A} = \frac{\mu}{4\pi}\vec{J}_\gamma \iiint_{v'} \frac{e^{-jk|\vec{r}-\vec{r'}|}}{|\vec{r}-\vec{r'}|} dv' \tag{44}$$

In our 1D case, we consider γ = x. The vector potential is written:

$$A_x = \frac{\mu}{4\pi} I_x \int_{-dx/2}^{dx/2} \frac{e^{-jk|\vec{r}-\vec{r'}|}}{|\vec{r}-\vec{r'}|} dx' \tag{45}$$

By applying the quasi-steady state approximation to equation (45), we therefore find:

$$A_x = \frac{\mu}{4\pi} I_x e^{-jkr} \int_{-dx/2}^{dx/2} \frac{1}{\sqrt{x^2+y^2+z^2}} dx' \tag{46 }$$

The calculation gives:

$$A_x = \frac{\mu}{4\pi} I_x e^{-jk} Log\left(\frac{x-\frac{dx}{2}+\sqrt{\left(x-\frac{dx}{2}\right)^2+y^2+z^2}}{x+\frac{dx}{2}+\sqrt{\left(x+\frac{dx}{2}\right)^2+y^2+z^2}}\right) \tag{47 }$$

The infinitesimally small dipole approximation is widely used in electromagnetic modeling especially in the field of antennas. In this case, the length of the dipole is infinitesimally small compared to the wavelength. Typically, it is less than a tenth. Note also that the distance of the observation point from the origin of the dipole is an important parameter in this approximation. The vector potential is written as:

$$A_x = \frac{\mu}{4\pi} I_x \frac{e^{-jkr}}{r} dx \quad (48)$$

To improve the calculation precision, we exploit the calculation approach based on the Maclaurin series. This approach is based on the fact that the length of the dipole is infinitely small compared to the wavelength. It resembles the infinitely small dipole approximation which is only a special case of it. Thus, we choose an order higher than the first order for calculation improvement.

By operating the change of variable ($\alpha = \frac{x'}{\lambda}, \eta = \frac{r}{\lambda}$ $et\ Q = \frac{x}{\lambda}$) in expression (45) and using relation (48), we obtain the integral expression of the potential vector, considering equation (49) below:

$$\frac{e^{-jk|\vec{r}-\vec{r'}|}}{|\vec{r}-\vec{r'}|} = \frac{e^{-jk\sqrt{(x-x')^2+y^2+z^2}}}{\sqrt{(x-x')^2+y^2+z^2}} \quad (49)$$

The new expression of the vector potential integrating the variable αis of the following form:

$$A_x = \frac{\mu}{4\pi} I_x \int_{-dx/2\lambda}^{dx/2\lambda} \frac{e^{-j2\pi\sqrt{\eta^2-2Q\alpha+\alpha^2}}}{\sqrt{\eta^2-2Q\alpha+\alpha^2}} d\alpha \quad (50)$$

Considering $\frac{e^{-j2\pi\sqrt{\eta^2-2Q\alpha+\alpha^2}}}{\sqrt{\eta^2-2Q\alpha+\alpha^2}} = f(\alpha)$, given that$\alpha \ll 1$ Taking into account the dimensions of discretization cells are very small compared to the wavelength, the development of the function $f(\alpha)$in the form of a Maclaurin series is in the following polynomial form:

$$f(\alpha) = f(0) + f'(0)\alpha + \frac{1}{2}f''(0)\alpha^2 + \frac{1}{6}f'''(0)\alpha^3 \quad (51)$$

Moreover, $f'(0) = f'''(0) = 0$because in the calculation of the integral of the polynomial equivalent to f between– *dx/2λ* and *dx/2λ* , terms of odd order, in particular those of the first and third order, are zero.

$$\vec{A}(x,y,z) = \frac{\mu}{4\pi} I_x \left(\frac{1}{2}f(0)\frac{dx}{\lambda} + \frac{1}{24}f''(0)\frac{dx^3}{\lambda^3}\right)\vec{e}_x \quad (52)$$

It is this last order which makes it possible to improve the precision. The component following o*x* of the vector potential is written, as in the case of the infinitely small dipole, as a function of the wavelength, of the length of the dipole. The expression of the vector potential is given by:

$$A_x = \frac{\mu}{4\pi} I_x e^{-jkr} dx \left(\left(\frac{1}{r} + \frac{1}{24r^3}\left(x^2(jkr)^2 + (3x^2 - r^2)(1 + jkr)\right)\right)dx^2\right) \quad (53)$$

Determining the radiation emissions of a cable system involves two main steps: calculating the conducted emissions and deducting the radiated emissions. The first step consists of determining the current passing through each discretization element. Then, using an analytical calculation method, the contribution of each discretization cell is determined based on the geometry and the current value at each frequency. The EM field at any point in space is the sum of the contributions of each cell, obtained by adding the different components of the magnetic and electric fields. The expressions of the latter are easily deduced from the expression (53).

3. Simulation Results

3.1 Declaration of Parameters

To carry out a realistic study and validate the algorithms developed above, we will consider the experimental data proposed in the works of (Wissem Yahyaoui, 2012), (Y. Ji and T. Hubing, 2000), (Martin Ludwig Zitzmann, 2007) and (Kenneth and L. Kaiser, 2004). To do this, by considering an electric dipole of length *dx=1cm*, carrying a current of *1A* and placing it at different points around this dipole, we vary the frequency from 0 to 10 GHz., $\mu_0 = 4\pi 10^{-7}$ and $\varepsilon_0 = 10^{-9}/36\pi$ (J. L. Volakis., A. Chatterjee., and L. C. Kempel, 1998). The vector potential will then be simulated at the coordinate points M (0.0.2) and M (0.0.5) cm. The simulation of the magnetic and electric fields generated by this dipole of length 1cm is done for a frequency equal to 550MHz, *1cm* above. If we take $N = 10^6$ for a dipole of length 1cm, we see that this chosen number is very high to ensure calculation accuracy.

3.2 Results

See Figures 6-17 below:

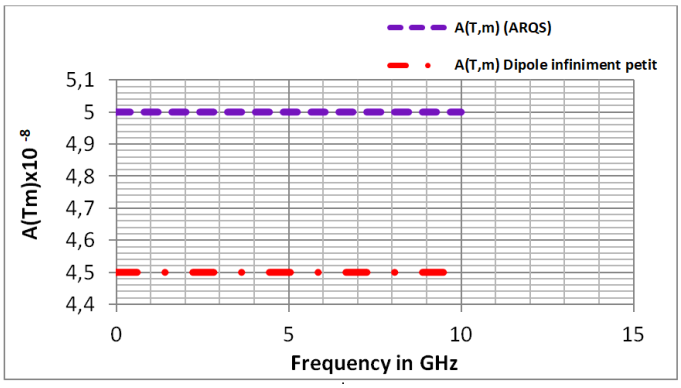

Figure 6. Vector potential at point M (0,0,2) : Simulation results

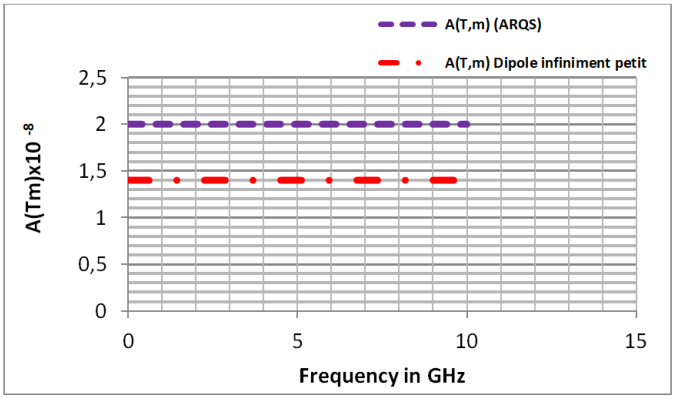

Figure 7. Vector potential at point M (0,0.5): Simulation results.

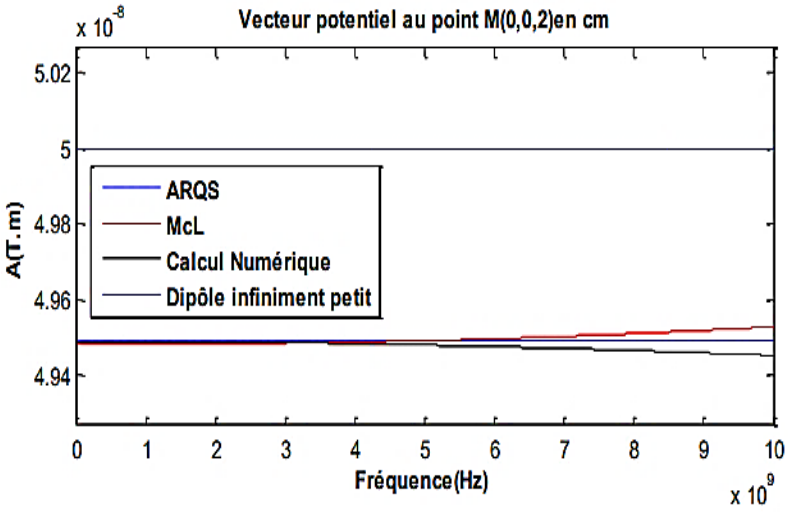

Figure 8. Modules of the vector potential at the point M (0,0,2) (Wissem Yahyaoui, 2012).

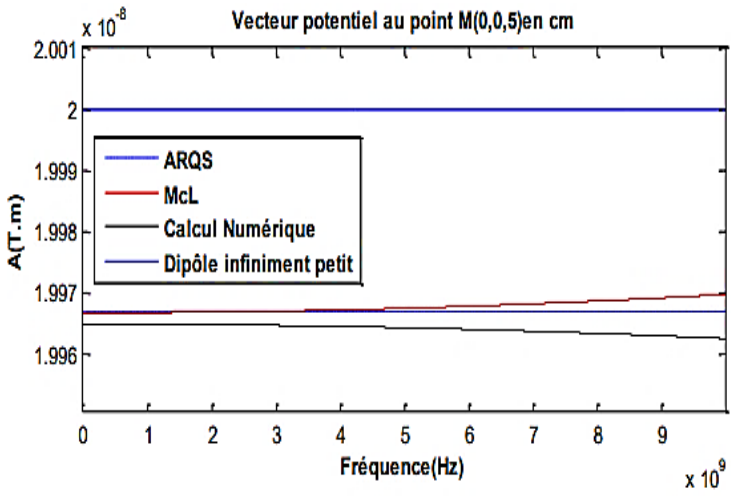

Figure 9. Modules of the vector potential at the point M (0,0.5) (Wissem Yahyaoui, 2012)

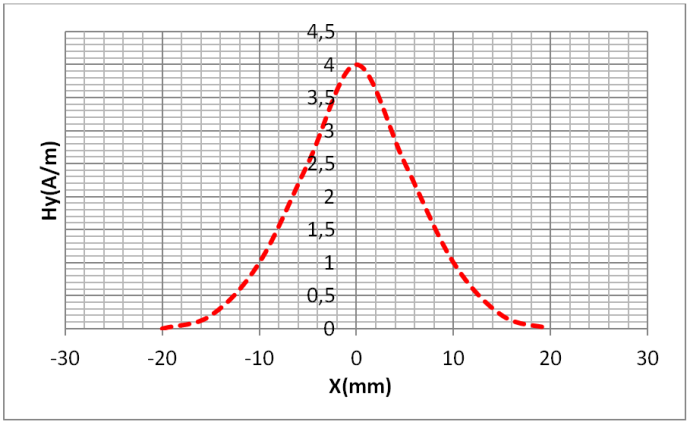

Figure 10. Profile of the magnetic field generated at 550MHz and 1cm above the current dipole 1A and length 1cm (the quasi-steady state approximation: ARQS). Simulation results.

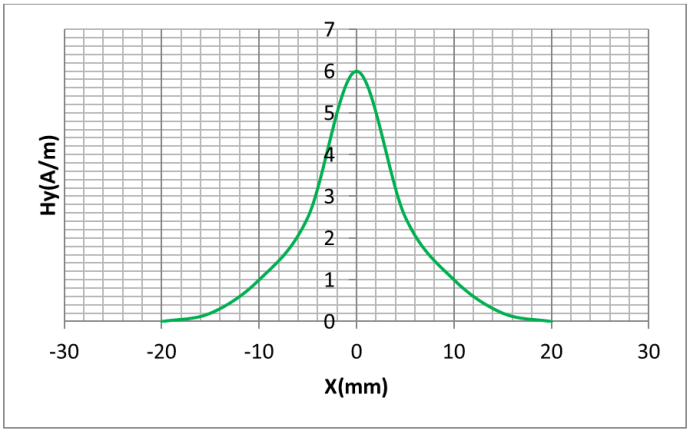

Figure 11. Profile of the magnetic field generated at 550MHz and 1cm above the dipole of current 1A and length 1cm (the infinitely small dipole approximation). Simulation results

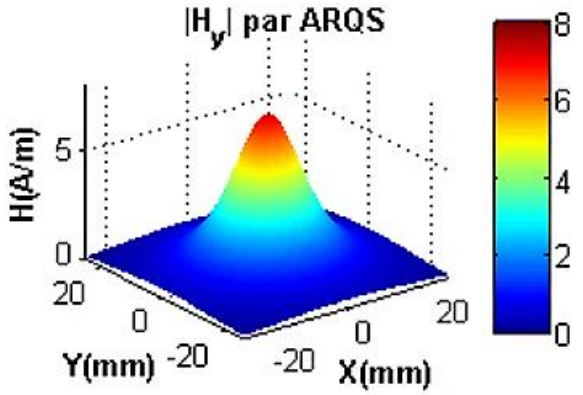

Figure 12. Profile of the magnetic field generated at 550MHz and 1cm above the current dipole 1A and length 1cm (the quasi-steady state approximation: ARQS). (Wissem Yahyaoui, 2012).

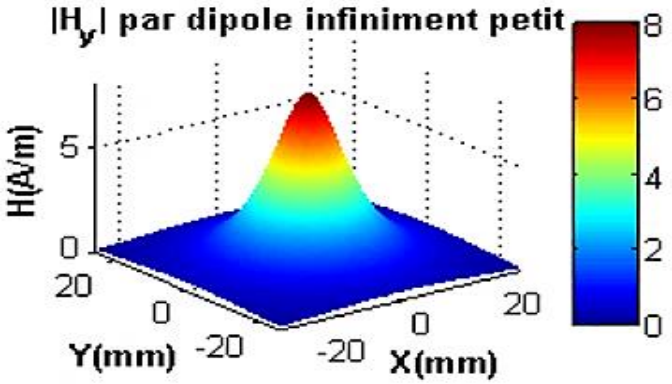

Figure 13. Profile of the magnetic field generated at 550MHz and 1cm above the dipole of current 1A and length 1cm (the infinitely small dipole approximation). (Wissem Yahyaoui, 2012)

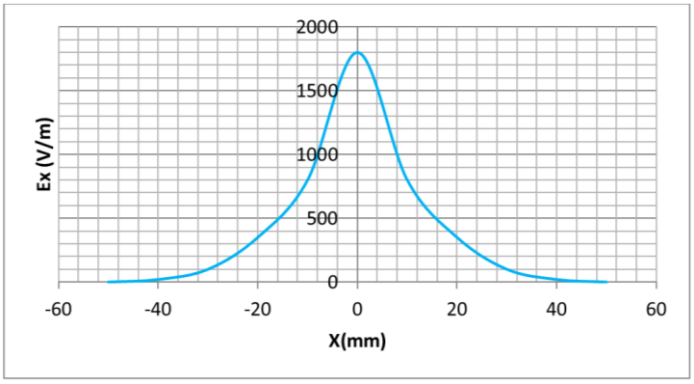

Figure 14. Profile of the electric field generated at 550MHz and 2cm above the current dipole 1A and length 1cm (Quasi-stationary regime approximation: ARQS) . Simulation results.

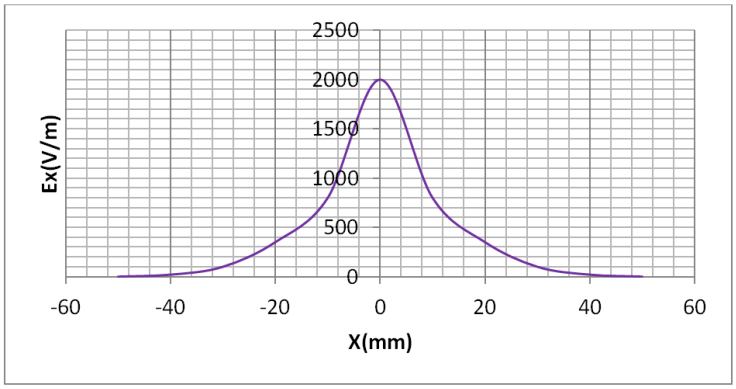

Figure 15. Profile of the electric field generated at 550MHz and 2cm above the dipole of current 1A and length 1cm (the infinitely small dipole approximation). Simulation results.

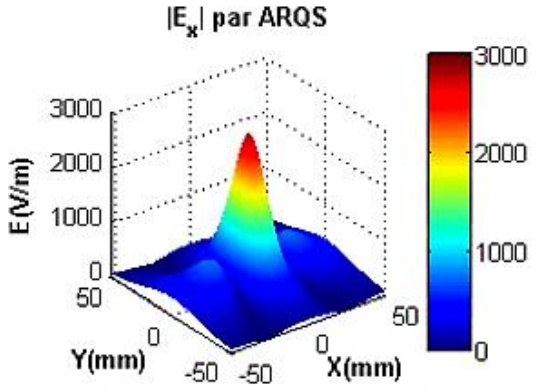

Figure 16. Profile of the electric field generated at 550MHz and 2cm above the dipole with current 1A and length 1cm. (Wissem Yahyaoui, 2012).

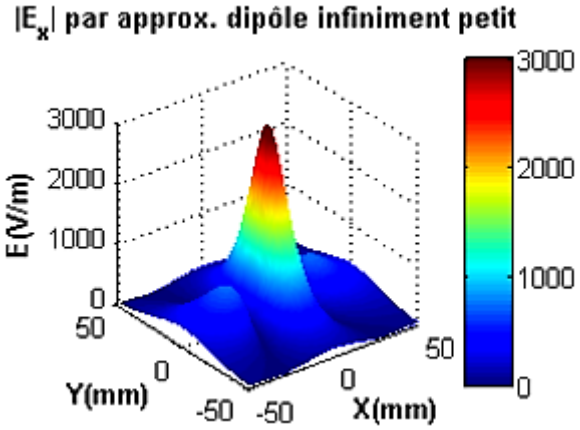

Figure 17. Profile of the electric field generated at 550MHz and 2cm above the dipole of current 1A and length 1cm (the infinitely small dipole approximation). (Wissem Yahyaoui, 2012)

4. Discussions of Results

The PEEC method is representative of these different phenomena which are conductor resistance, inductances, mutual inductances (or inductive coupling), skin effect, and proximity effect. In this study, skin and proximity effects were not considered because of the small section of the cables studied, the crosstalk between power and control cables as well as the approximation taking into account the three dimensions of the cells. discretization was not also taken into consideration. However, these factors can modify the proposed PEEC model and

influence the precision of the forecasts made as soon as we increase the frequency. For radiated emissions, however, the calculation remains valid for any structure as long as the PEEC method is correctly adapted.

The 2D simulation results based on the proposed models and on the experimental parameters taken from the work of (Wissem Yahyaoui, 2012) are as follows:

Figures 6 and 7 show the profile of the vector potential calculated at the points (0.0.2) and (0.0.5) cm by the quasi-steady state approximation and the infinitely small dipole approximation. These curves demonstrate that the evolution of the vector potential is a constant function of the frequency. At the points (0.0.2) and (0.0.5) cm the two approximations give rise respectively to the vector potentials of (5 Tm and 4.5 Tm) and (2 Tm and 1.4 Tm). These results are close to those presented in Figures 8 and 9 from the work of (Wissem Yahyaoui, 2012) with a relative deviation rate associated with the infinitely small dipole approximation of 0.1 or 10% at the point (0 .0.2) cm compared to the results in Figure 8 and 0.2 or 20% compared to the results presented in Figure 9.

Figures 10 and 11 give the spatial profile of the magnetic field radiated by the on-board electronic cabling system as a function of the distance obtained by the quasi-stationary regime approximation and the infinitely small dipole approximation. These two approximations show that the intensity of the radiated magnetic field is greater the closer we get to the conductor with a respective amplitude of 4 A/m and 6A/m. By virtue of the Maxwell-Ampère theorem, this radiated magnetic field can induce, by magnetic coupling, pulses of disruptive currents di/dt in nearby systems. This intensity decreases as we move away from the cable. These results are comparable to those of Figures 12 and 13 taken from the experimental work proposed by (Wissem Yahyaoui, 2012).

Finally, Figures 14 and 15 present the spatial distribution of the electric field radiated by the on-board electronic wiring system obtained by the quasi-stationary regime approximation and the infinitely small dipole approximation. These two approximations show that the intensity of the electric field is of very high amplitude near the conductor, i.e. 1800 V/m and 2000 V/m respectively. By virtue of the Maxwell-Faraday theorem, this intensity of the radiated field is capable of inducing by electrical coupling the disturbing voltage pulse dv/dt in the neighboring system. These results are similar to those of Figures 16 and 17 obtained experimentally in the work of (Wissem Yahyaoui, 2012) but with a relative deviation rate of 0.02 or 2% observed in the results of Figure 16 compared to those of the Figure 14.

The temporal variations of the induced current and voltage modeled by *di/dt* and *dv/dt* constitute the basis of electromagnetic pollution. In LF, these variations cause so-called harmonic disturbances and in HF, they are the basis of electromagnetic interference. In this context, modeling radiated EM emissions constitutes a great challenge, especially since these emissions represent an enormous risk for the proper functioning of systems and for EMC approval.

To minimize the risks of harmonic disturbances and EM interference with other devices and in particular with control devices, it is necessary to first predict the EM emissions generated and then limit the disturbances harmful to operation and the security of the overall system. Therefore, it is important to predict the conducted and radiated emissions of cables which are, by their large size, a potential EM risk for the surrounding electronic system by advocating the need to separate the power cables from the control cables. We can also do EMC filtering which is an interesting and more popular solution in the embedded electronic system industry.

Indeed, EM modeling itself requires a combination of several numerical methods. It depends on the dimensions and especially the geometry. So, the choice of an appropriate EM modeling method for each substructure or the combination of several methods is a possible solution but remains very delicate. Furthermore, to integrate this EM phenomenon into the model of embedded electronics, we need an electrical model of the EM behavior of the most radiating structures such as bus bars, cables and ground planes.

The PEEC method is representative of these different phenomena which are conductor resistance, inductances, mutual inductances (or inductive coupling), skin effect, and proximity effect. In this study, skin and proximity effects were not considered because of the small section of the cables studied, the crosstalk between power and control cables as well as the approximation taking into account the three dimensions of the cells. discretization was not also taken into consideration. However, these factors can modify the proposed PEEC model and influence the precision of the forecasts made as soon as we increase the frequency. For radiated emissions, however, the calculation remains valid for any structure as long as the PEEC method is correctly adapted.

5. Conclusions

Therefore, the electromagnetic disturbances generally generated by power electronic systems, and which mainly come from electrical machines, high frequency cutting and electrical cables, although these electromagnetic

disturbances depend enormously on the dimensions of the sources. Since cables are the longest structures and also the best antennas of electromagnetic radiation in embedded electronic systems, if the dimensions of electronic circuits are negligible compared to cables. The emissions radiated by the latter can propagate towards control systems which are often designed with increasingly vulnerable components. This vulnerability is mainly due to miniaturization, the increase in operating frequency and the decrease in supply voltage.

Nowadays, modeling radiated EM emissions from embedded electronic systems constitutes a great challenge because these emissions represent an enormous risk for the proper functioning of the systems and also for EMC approval. The difficulty of accounting for this phenomenon linked to this system is obvious which is accentuated by the strong electronic integration. Because, it depends on the dimensions and especially the geometry as we have highlighted.

Thus, the choice of an appropriate EM modeling method for each structure depends on the combination of several methods which is a possible solution but remains very delicate.

In order to limit the risk of electromagnetic interference with other devices and in particular with control devices, this article is part of the context of modeling the prediction of EM emissions radiated by on-board electronic cabling systems.

The 2D simulation results obtained based on the proposed models demonstrate that the evolution of the vector potential is constant whatever the frequency, while the spatial distribution of the intensity of the electromagnetic field radiated by the on-board electronic cabling system is all the more important as one is close to the conductor with a high probability of inducing by electromagnetic coupling the pulses of currents and voltages due to neighboring systems. This intensity decreases as we move away from the cable. These current and voltage pulses constitute the basis of electromagnetic pollution and cause so-called harmonic disturbances and EM interference.

To optimize the risks of harmonic disturbances and EM interference with other devices and in particular with control devices, we recommend taking into account the prediction of radiated EM emissions from the design of on-board electronic systems to minimize harmful disturbances. The operation and safety of the overall system. Therefore, it is important to predict the conducted and radiated emissions of cables which are, by their large size, a potential EM risk for the surrounding electronic system by advocating the need to separate the power cables from the control cables. We also recommend EMC filtering which is an interesting and more popular solution in the embedded electronic system industry.

The simulation of the electric field from currents gives good results. In certain cases, when the capacitive effect predominates over the inductive effect, the distribution of the current circulating in the cable becomes discontinuous. This discontinuity also affects the calculation of the electric field; the sudden change in the direction of the current in the cable modifies the calculation of the electric field. This is why it is necessary to calculate the electric field not from the current, but from the surface charges, which can be deduced from the voltages obtained by the PEEC method. A new perspective on the prediction of radiated emissions should take into account the skin effect, the proximity effect, the crosstalk between power cables and those of control as well as the approximation taking into account the three dimensions of the cells of authors including discretization of natural environmental and socio-economic factors in order to improve the PEEC model and circumvent the influence on the precision of the results.

Acknowledgments

I personally thank colleagues who helped critique the manuscript. Also, those who participated in the review and acceptance of this article:

- Evaluators or editors,

- Associate editors

- Consulting editors of the journal in which the article is to appear.

I greatly appreciate the valuable contributions of the members of your community advisory committee including the team members who took part in participating in this study.

Not knowing the names of members of your newspaper, I would like to thank all your associates. Finally, I personally thank my entire team who support me in the research (my assistants, secretary, software and simulation manager, etc.).

Authors contributions

I would like to inform your journal that this article did not have the contribution of other authors except the

reviewers who were able to make a relevant contribution during the examination of the article.

Funding

I would like to inform your journal that the financing of this article is done with my own means.

Competing interests

I declare that there are no known competing financial interests or personal relationships that could appear to influence the work reported in this article.

Informed consent

Obtained.

Ethics approval

The Publication Ethics Committee of the Canadian Center of Science and Education.

The journal's policies adhere to the Core Practices established by the Committee on Publication Ethics (COPE).

Provenance and peer review

Not commissioned; externally double-blind peer reviewed.

Data availability statement

The data that support the findings of this study are available on request from the corresponding author. The data are not publicly available due to privacy or ethical restrictions.

Data sharing statement

No additional data are available.

References

A. E. Ruehli. (1972). Inductance Calculations in a Complex Integrated Circuit Environment. *IBM Journal of Research and Development, 16(*5), 470-481. https://doi.org/10.1147/rd.165.0470

A. E. Ruehli., & P. A. Brennan. (1973). Efficient Capacitance Calculations for Three-Dimensional Multiconductor Systems. *IEEE Transactions on Microwave Theory and Techniques, 21*(2), 76-82. https://doi.org/10.1109/TMTT.1973.1127927

A. E. Ruehli., G. Antonini., & A. Orlandi. (1999). *Extension of the Partial Element Equivalent Circuit Method to Non Rectangular Geometries*. in Proceeding. of the Int. Symposium on EMC, pages 728-733, Seattle, Washington, USA. https://doi.org/10.1109/ISEMC.1999.810108

A. Müsing., J. Ekman., & J.W. Kolar. (2009). Efficient Calculation of Non-Orthogonal Partial Elements for the PEEC Method. *IEEE Transactions on Magnetics, 45*(3), 1140-1143. https://doi.org/10.1109/TMAG.2009.2012655

A. Ruehli. (1974). Equivalent circuit models for three dimensional multiconductor systems. *IEEE Transactions on Microwave Theory and Techniques, 22*(3), 216-221. https://doi.org/10.1109/TMTT.1974.1128204

A. Ruehli., & H. Heeb. (1992). Circuit models for three-dimensional geometries including dielectrics. *IEEE Trans. Microwave Theory Tech., 40,* 1507-1516. https://doi.org/10.1109/22.146332

Acharf, L. (2017). *Analysis and modeling of the electromagnetic radiation of PLC networks*. Thèse de doctorat, Université Clermont Auvergne (2017-2020) en cotutelle avec Université Sidi Mohamed ben Abdellah (Fès, Maroc). Retrieved from https://theses.fr/2017CLFAC063

Amadou, B. D. (2023). *Co-simulation for EMC Modeling of Complex Electrical Systems*. Thesis to obtain the degree of Doctor from the University of Lyon carried out within the École Centrale de Lyon Specialty: Electrical Engineering AMPÈRE Laboratory Doctoral School N◦ 160 Electronics, Electrotechnics, Automatics.

C. Ho., A. Ruehli., & P. Brennan. (1975). *The Modified Nodal Approach to Network Analysis*. IEEE Trans. Circuits Syst., pp. 504-509. https://doi.org/10.1109/TCS.1975.1084079

C.-S. Yen., Z. Fazarinc., & R. L. Wheeler. (1982). Time-Domain Skin-Effect .Model for Transient Analysis of Lossy Transmission Lines. *Proceedings of the IEEE, 70*, 750-757. https://doi.org/10.1109/PROC.1982.12381

Constantine., & A. Balanis. (1996). *Antenna Theory: Analysis And Design* (2nd ed.).

Cyril, B. (2004). *Contribution to design through simulation in power electronics: application to the low voltage inverter*. PhD thesis National Institute of Applied Sciences of Lyon.

E. Clavel. (1996). *Towards a cabling design tool: INCA software*. Doctoral Thesis, Institut National Polytechnique de Grenoble.

E.Vialardi. (2003). "*An order reduction technique coupled with PEEC models: application on aeronautical equipment*", Doctoral thesis from Politechnico de Torino.

European Directive. (1989). of the European Parliament and the Council, May 3.

European Directive. (2004). of the European Parliament and the Council, December 15.

F. A. Kharanaq, A. Emadi, & B. Bilgin. (2020). Modeling of conducted emissions for emi analysis of power converters: State-of-the-art review. *IEEE Access, 8*, 189313-189325. https://doi.org/10.1109/ACCESS.2020.3031693

F. Duval. (2007). *Management of electrical mass wiring in a motor vehicle: CEM application*. Doctoral Thesis, University of Paris Sud XI.

F. Duval. (2007). *Management of electrical mass wiring in a motor vehicle: CEM application*. Doctoral Thesis, University of Paris Sud XI.

G. Antonini., & A. Ruehli. (2003). *On Modeling Accuracy of EMI Problems using PEEC*. Proc of IEEE International Symposium on EMC, Boston, USA.

G. Antonini., A. E. Ruehli., J. Esch., J. Ekman., A. Mayo., & A. Orlandi. (2003). Nonorthogonal PEEC Formulation for Time- and Frequency-Domain EM and Circuit Modeling. *IEEE Transactions on Electromagnetic Compatibility, 45*(2), 167-176. https://doi.org/10.1109/TEMC.2003.810804

G. Antonini., J. Ekman., & A. Orlandi. (2003). "*3D PEEC capacitance calculations*", Proceedings of the IEEE International Symposium on EMC, Boston, USA, pp. 630–635.

G. Wollenberg., & S. V. Kochetov. (2003). *Modeling the skin effect in wire-like 3D interconnection structures with arbitrary cross section by a new modification of the PEEC method*. in Proceeding of 15th Int. Symp. on Electromagn. Compat., Zürich, Switzerland, pp. 609–614.

I. Yahi. (2009). *Modeling of radiation sources within a motor vehicle taking into account the presence of the ground plane*. Doctoral thesis, University of Rouen.

I. Yahi., F. Duval., & A. Louis. (2007). *A New Capacitive Coupling Consideration in PEEC Method* 2emc Symposium on embedded EMC.

J. Ekman & S. Niska. (2004). *Combining 2D Transmission Line Models with 3D PEEC Models*. in Proceeding of EMB04, Gothenburg, Sweden.

J. Ekman. (2003). *Electromagnetic Modeling using the Partial Element Equivalent Circuit Method*. PhD Dissertation, EISLAB: Embedded Internet System Laboratory, Computer Science and Electrical Engineering, Lulea University of Technology.

J. Ekman. (2003). *Electromagnetic Simulations Using The Partial Element Equivalent Circuit (PEEC) Approach*. in Proceeding of Progress in Electromagnetics Research Symposium, Honolulu, HI, USA, 13-16.

J. Ekman., & G. Antonini. (2004). *On Characterizing Artifacts Observed in PEEC Based Modeling*. in Proceeding of the IEEE International Symposium on Electromagnetic Compatibility, Santa Clara, CA, USA. https://doi.org/10.1109/ISEMC.2004.1350035

J. Ekman., & Lundgren, U. (2001). *Analysis of printed antenna structures using the partial element equivalent circuit (PEEC) method*. Conference proceedings: electromagnetic computations - methods and applications. - Uppsala, Sweden.

J. Garrett., A. E. Ruehli., & C. R. Paul. (1998). Accuracy and Stability Improvements of Integral Equation

Models using the Partial Element Equivalent Circuit (PEEC) Approach. *IEEE Trans. Antennas Propagat., 46*(12), 1824-1831. https://doi.org/10.1109/8.743819

J. Jin., & J. Douglas. (2009). *Finite Element Analysis of Antennas and Arrays*. Wiley-IEEE. https://doi.org/10.1002/9780470409732

J. L. Volakis., A. Chatterjee, & L. C. Kempel. (1998). *Finite element method for electromagnetism: antennas, microwave circuits and scattering applications*. IEEE Press Series on Electromagnetic Wave Theory. https://doi.org/10.1109/9780470544655

Jack Vanderlinde. (2005). "*Classical Electromagnetic Theory* (2nd ed.). Kluwer Academic Publishers, New York. https://doi.org/10.1007/1-4020-2700-1

Jean-Marc, D. (2010). *Rob-cem I: a complete introduction to electromagnetic compatibility issues in embedded electronic circuits and architectures*.

Jean-Paul Gonnet. (2005). *Optimization of electrical conduits and distribution cabinets*. Doctoral thesis of Joseph University.

K. Kadem, M. Bensetti, Y. Le Bihan, E. Labouré, & M. Debbou. (2021). Optimal coupler topology for dynamic wireless power transfer for electric vehicle. *Energies, 14*(13). https://doi.org/10.3390/en14133983

K. Kadem. (2020). *Modeling and optimization of a magnetic coupler for dynamic induction charging of electric vehicles*. PhD thesis, University Paris Saclay, 2020. Doctoral thesis supervised by Labouré Eric in Electrical Engineering.

K. M Coperich., A. E. Ruehli., & A. Cangellaris. (2000). Enhanced Skin Effect for Partial Element Equivalent Circuit (PEEC) Models. *IEEE Transactions Microwave Theory and Technique, 48,* 1435-1442. https://doi.org/10.1109/22.868992

Kenneth., & L. Kaiser. (2004). *Electromagnetic Compatibility Handbook: Circuits, Signals and Systems*. Chapter 3, CRC Press.

L. Di Leonardo, M. Popescu, M. Tursini, & M. Villani. (2019). Finite elements model co simulation of an induction motor drive for traction application. *in IECON 2019 45th Annual Conference of the IEEE Industrial Electronics Society, 1,* 1059-1065. https://doi.org/10.1109/IECON.2019.8926853

M. Enohnyaket & J. Ekman. (2009). Analysis of air-core reactors from dc to very high frequencies using PEEC models. *IEEE Transactions on Power Delivery, 24*(2), April. https://doi.org/10.1109/TPWRD.2009.2014486

M. Enohnyaket. (2007). PEEC Modeling and Verification for Broadband Analysis of Air-Core Reactors. Licentiate Thesis Luläa University of Technology, 2007.

M. W. Ali., T. H. Hubing., & J. L. Drewniak. (1997). A hybrid FEM/MoM technique for electromagnetic scattering and radiation from dielectric objects with attached wires. *IEEE Transactions on Electromagnetic Compatibility, 39,* 304-314. https://doi.org/10.1109/15.649818

M.N.O. Sadiku. (1994). *Elements of Electromagnetics*. New York: Oxford Univ.

Martin, L. Z. (2007). *Fast and Efficient Methods for Circuit-based Automotive EMC Simulation*. Thèse de doctorat de l'université de Nürnberg, Allemagne.

Mathias, E. (2007). *PEEC Modeling and Verification for Broadband Analysis of Air Core Reactors*. dissertation of PhD from University of Technology lulea, Sweden.

Mr. Besacier. (2001). *Adaptation of the PEEC method to the electrical representation of power electronics structures*. Doctoral Thesis, Institut National Polytechnique de Grenoble.

Mr. Toure. (2019). *Contribution to the CEM modeling of an actuation chain for an automotive application*. Theses, Clermont Auvergne University.

Roger, F., & Harrington. (2015). "*Time Harmonic Electromagnetic Fields*" by IEEE Press series on electromagnetic wave theory.

S. Mei., & Y. Ismail. (2003). *Modeling skin effect with reduced decoupled R-L circuits*. International Symposium on Circuits and Systems, Thailand, pages 588-591, 2003. https://doi.org/10.1109/ISCAS.2003.1206150

S. Mei., & Y. Ismail. (2004). Modeling Skin and Proximity Effects With Reduced Realizable RL Circuit. *IEEE Transactions On Very Large Scale Integration (VLSI) Systems, 12*(4), 437-447, April. https://doi.org/10.1109/TVLSI.2004.825863

Sergey V. Kochetov. (2008). *Time- and frequency-domain modeling of passive interconnection structures in field and circuit analysis*. rapport de habilitation.

T. Hubing. (1991). *Survey of Numerical Electromagnetic Modeling Techniques*. Department of Electrical Engineering, University of Missouri-Rolla, USA.

T. K. Mersha & C. Du. (2022). Co-simulation and modeling of pmsm based on ansys software and simulink for evs. *World Electric Vehicle Journal*, *13*(1). https://doi.org/10.3390/wevj13010004

T. V. Dinh., B. Cabon., & J. Chilo. (1990). New skin-effect equivalent circuit. *Electronic Letters, 26,* 1582-1584. https://doi.org/10.1049/el:19901015

Tran Thanh Son. (2008). "*Coupling the finite element method with the PEEC method: application to the modeling of electromagnetic devices including complex conductor systems*" doctoral thesis from Joseph Fourier University.

Tran, T. S. (2008). *Coupling the finite element method with the PEEC method: application to the modeling of electromagnetic devices including complex conductor systems*. doctoral thesis from Joseph Fourier University.

Tristan, D. (2009). *Study of the effect of electromagnetic waves on the operation of electronic circuits - Implementation of a method for testing electronic systems.* Montpellier II Science and Technology University of Languedoc.

V. Varvolik, D. Prystupa, G. Buticchi, S. Peresada, M. Galea, & S. Bozhko. (2021). Co simulation analysis for performance prediction of synchronous reluctance drives. *Electronics*, *10*(17). https://doi.org/10.3390/electronics10172154

W. Wang, X. Fang, H. Cui, F. Li, Y. Liu, & T. J. Overbye. (2022). Transmission-and distribution dynamic co-simulation framework for distributed energy resource fre quency response. *IEEE Transactions on Smart Grid*, *13*(1), 482-495. https://doi.org/10.1109/TSG.2021.3118292

Wenns, Y. (2006). Modeling of energy cables subject to constraints generated by electronic power converters. Thesis for obtaining a Doctorate from the University of Science and Technology of Lille, Department of Electrical Engineering. Retrieved from https://theses.fr/2006LIL10104

Wissem, Y. (2012). *Characterization and modeling of emissions radiated by the wiring of on-board electronic systems.* Doctoral thesis defended at the Doctoral School “Information Sciences and Technologies, Telecommunications and Systems. Retrieved from https://theses.hal.science/tel-00737499/document

Y. J. Hwang & J. Y. Jang. (2020). Design and analysis of a novel magnetic coupler of an in-wheel wireless power transfer system for electric vehicles. *Energies*, *13*(2). https://doi.org/10.3390/en13020332

Y. Ji & T. Hubing. (2000). EMAP5: A 3D Hybrid FEM/MOM Code. *Journal of the Applied Computational Electromagnetics Society, 15*(1), 1-12.

Yu Z. (2006). *Multigrid Finite Element Methods For Electromagnetic Field Modelling*. IEEE Press Series on Electromagnetic Wave Theory.